The Era of Multi-Messenger Solar Physics
Proceedings IAU Symposium No. 372, 2023
G. Cauzzi & A. Tritschler, eds.
doi:10.1017/S1743921323000509

Automatic detection of solar active regions from SOHO/MDI and SDO/HMI synoptic magnetograms

Ruihui Wang[1,2], Jie Jiang[1,2] and Yukun Luo[1,2]

[1]School of Space and Environment, Beihang University, Beijing, China

[2]Key Laboratory of Space Environment monitoring and Information Processing of MIIT, Beijing, China

Abstract.
We develop an adaptive method to automatically identify ARs from radial synoptic maps observed by SOHO/MDI and SDO/HMI, calibrate the detections between HMI and MDI data based on identified ARs flux and area and further derive a homogeneous dataset including ARs' area and flux over the last two solar cycles. The data are compared with sunspot number, USAF/NOAA sunspot area, SMARPs and SHARPs and BARD area and flux, which show reasonable agreement. The identified ARs during the overlap period of MDI and HMI have the same areas as a whole while the AR flux based on MDI maps is about 1.36 times as large as that of HMI maps. Based on our dataset, we find strong ARs ($|flux| > 10^{22}$Mx) contribute most to the difference between cycles 23 and 24 while other ARs ($|flux| < 10^{22}$Mx) are similar in the two cycles in both area and flux.

Keywords. Sun: activity, Sun: magnetic fields, techniques: image processing

1. Introduction

Solar active regions (ARs) play an essential role in solar physics. They not only provide insight into the solar dynamo but also lead to long and short-term solar variability. In this work, we aim to develop a new method to automatically detect ARs from SOHO/MDI and SDO/HMI radial synoptic magnetograms and to provide a new database of ARs between 1996 and 2020.

2. Method

The latitude range of detection is limited to ±60°. There are five modules in the detection algorithm. The first module is adaptive threshold segmentation to remove the background magnetic fields with different thresholds in different pixels. The second module is morphological closing operation and opening operation to remove small magnetic segments and get the ARs' kernel pixels, which are used as seeds in region growing. The third module is region growing to get all pixels of each single AR. All pixels connected to the seeds and stronger than the threshold are recovered. The fourth module is closing operation and removing decayed ARs segments that are smaller than an area threshold. The fifth module is merging neighbor regions and removing unipolar regions. We use dilation operation to merge separate segments and drop all unipolar ARs whose flux imbalance is greater than 50%.

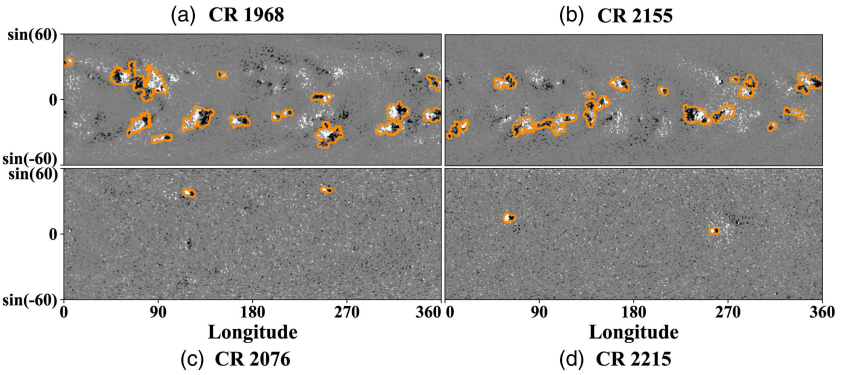

Figure 1. Examples of the detected ARs based on synoptic magnetograms. MDI (left) and HMI (right) at different phases of cycles 23 and 24 are used to demonstrate the accuracy of the algorithm. The 4 magnetograms are overplotted with the contours in dark orange outlining the perimeter of the detected ARs.

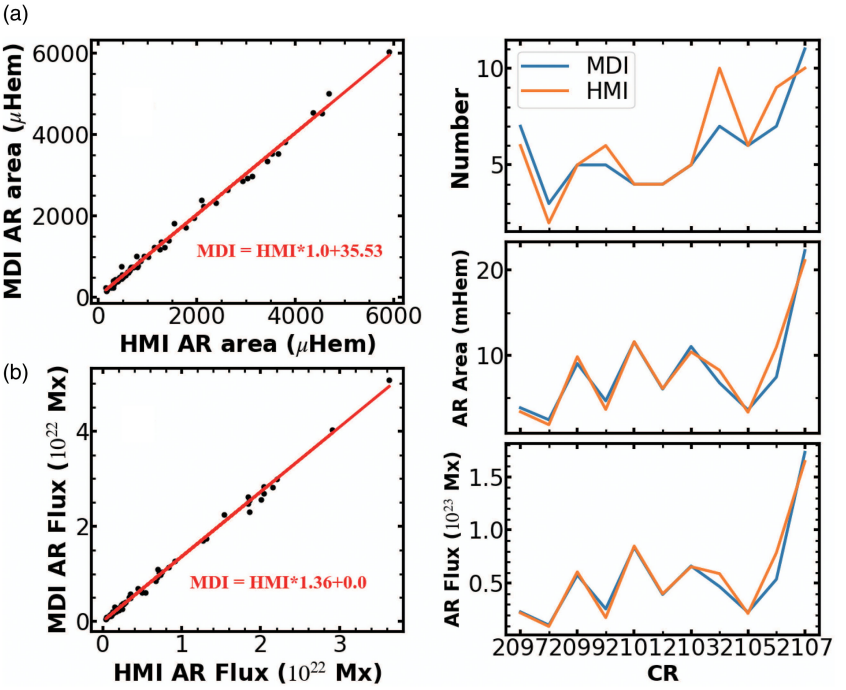

Figure 2. Calibration of the detected results based on MDI and HMI magnetograms and comparison of detected ARs during the 11 HMI and MDI overlap CRs. The ARs flux in right bottom panel is calibrated results.

3. Calibration, Validation and Statistics

Since MDI and HMI synoptic magnetograms have different resolutions, we use the magnetograms during the overlap period to calibrate the parameters used in HMI magnetograms to obtain the same ARs detections as in MDI magnetograms. The detection results during the overlap period show great agreement after calibration.

https://doi.org/10.1017/S1743921323000509 Published online by Cambridge University Press

After calibration, we obtain the homogeneous ARs dataset including location, area, and flux for cycles 23 and 24. The dataset is evaluated by comparing it with other datasets, i.e., sunspot number, USAF/NOAA sunspot area, SMARPs and SHARPs (Bobra et al. (2021), Bobra et al. (2014)) area and flux, and BARD (Muñoz-Jaramillo et al. (2016)) area and flux.

We divide ARs into three categories based on their unsigned flux and find that although cycle 24 is about twice weaker than cycle 23 based on the sunspot number, the numbers and total flux of median and weak ARs in the two cycles are almost the same.

Acknowledgements

The SDO/HMI data are courtesy of NASA and the SDO/HMI team. SOHO is a project of international cooperation between ESA and NASA. The research is supported through the National Natural Science Foundation of China (grant Nos. 12173005 and 11873023).

Supplementary material

To view supplementary material for this article, please visit https://doi.org/10.1017/S1743921323000509.

References

Bobra, M. G., Sun, X., Hoeksema, J. T., et al. 2014, Sol Phys, 289, 3549

Bobra, M. G., Wright, P. J., Sun, X., & Turmon, M. J. 2021, APJS, 256, 26

Muñoz-Jaramillo, A., Werginz, Z. A., Vargas-Acosta, J. P., et al. 2016, in 2016 IEEE International Conference on Big Data (Big Data), 3194–3203